Applied Energy 155 (2015) 637–647

Contents lists available at ScienceDirect

Applied Energy

journal homepage: www.elsevier.com/locate/apenergy

Biodiesel production direct from high acid value oil with a novel magnetic carbonaceous acid

Fan Zhang [a,b], Zhen Fang [a,*], Yi-Tong Wang [a,b]

[a] Chinese Academy of Sciences, Biomass Group, Key Laboratory of Tropical Plant Resources and Sustainable Use, Xishuangbanna Tropical Botanical Garden, 88 Xuefulu, Kunming, Yunnan Province 650223, China
[b] University of Chinese Academy of Sciences, 19A Yuquan Road, Beijing 100049, China

HIGHLIGHTS

- A novel route with five steps to produce a new magnetic carbonaceous acid.
- The catalyst has high acid content (2.79 mmol/g) and magnetism (14.4 Am^2/kg).
- 91.8% *Jatropha* biodiesel yield is achieved with the catalyst directly.
- The catalyst is stable for 3 cycles with biodiesel yield >90% at AV of 17.2.
- The recovery rate of catalyst is 96.3% after 3 cycles.

GRAPHICAL ABSTRACT

A novel magnetic carbonaceous acid catalyst was synthesized from glucose and iron chloride by a new method of double hydrothermal precipitation and pyrolysis, and subsequent sulfonation. The catalyst presents high active, stable and recoverable in the production of *Jatropha* biodiesel with high yields for 3 cycles (90.5%, 91.8%, 90.3%), slight reduction in total acid density (2.43 *vs.* 2.79 mmol/g) and high catalyst recovery rate of 96.3%.

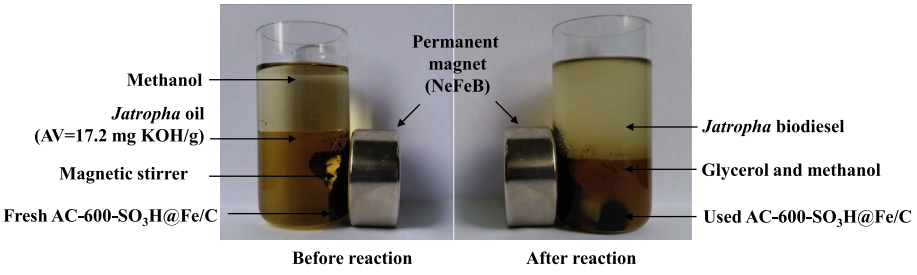

ARTICLE INFO

Article history:
Received 15 April 2015
Received in revised form 8 June 2015
Accepted 17 June 2015
Available online 1 July 2015

Keywords:
Biodiesel
High acid value
Magnetic carbonaceous acid
Hydrothermal
Sulfonation

ABSTRACT

A novel magnetic carbonaceous acid catalyst was synthesized from glucose and iron chloride by a new method of double hydrothermal precipitation at 180 °C and pyrolysis at 400–800 °C, and subsequent sulfonation at 150 °C. Its crystalline phases, magnetic saturation (Ms), morphology, specific surface area, pore volume, functional groups, thermal stability, elemental composition and total acid density were analyzed with various techniques. It was found that catalyst carbonized at 600 °C (AC-600-SO_3H@Fe/C) had high acid density (2.79 mmol/g) and strong magnetism (Ms: 14.4 Am^2/kg) for direct production of biodiesel from *Jatropha* oil with high acid value (17.2 mg KOH/g) by single-factor optimization. With the catalyst, 90.5% biodiesel yield was achieved at 200 °C with 3 cycles (>90% yield) and 96.3% catalyst recovery rate. The magnetic catalyst directly esterified and transesterified high acid value oil without pretreatment with high biodiesel yield and easily separated for three recycles with little deactivation. It could also find other applications such as pretreatment of oils with high AV and hydrolysis of biomass.

1. Introduction

Due to limited fossil resources and greenhouse gas emissions caused by the combustion of fossil fuels, the researches for converting renewable biomass to alternative fuels have gained much attention [1,2]. Biodiesel [3] is considered as a good alternative

* Corresponding author. Tel.: +86 871 65137468; fax: +86 871 65160916.
E-mail address: zhenfang@xtbg.ac.cn (Z. Fang).
URL: http://brg.groups.xtbg.ac.cn/ (Z. Fang).

http://dx.doi.org/10.1016/j.apenergy.2015.06.044
0306-2619/

for fossil fuels because it is clean, renewable and carbon neutral [4]. Biodiesel production by transesterification catalyzed by base heterogeneous catalysts, such as modified CaO [5], KF/γ-Al_2O_3/honeycomb [6] and sodium silicate [7] are widely studied because they are easier recovered than homogeneous ones [8]. However, the technology based on these base catalysts requires using crude oils with low free fatty acids (FFAs) to avoid saponification [9]. So, solid acid catalysts, such as macroporous cation exchange resin [10], heteropoly acid [11] and sulfonated metallic oxides (e.g., zirconia, tin and titanium oxide) [12–14] are studied to produce biodiesel from high FFA oils.

Sulfonated activated carbon (AC-SO_3H) can also catalyze both esterification and transesterification to produce biodiesel from oils with high acid value (AV) without pretreatment [15,16]. Because, AC has properties like its surface oxides [17], reducibility [18], and stability in both acidic and basic media [19], as well as its structural resemblance to graphite [20], fullerenes [21] and nanotubes [22] to support —SO_3H well. However, the separation of AC-SO_3H catalyst needs filtration or centrifugation [23] that is energy and time consuming. So, many magnetic carbonaceous acids were successfully prepared that are easily separated by a magnet, such as Fe_3O_4@C-SO_3H [24], magnetic lignin-derived amorphous carbon solid acid (MLC-SO_3H) [25] and sulfonated magnetic carbon nanotube arrays (sulfonated MCNAs) [26] for cellulose hydrolysis, fructose dehydration and hydrolysis of polysaccharides in crop stalks (Table 1). But these catalysts have low acid content (1.3, 1.95 and 0.38 mmol/g) for effective biodiesel production, some have low magnetism [e.g., for sulfonated MCNAs with only magnetic saturation (Ms) of 6.32 Am^2/kg before sulforation].

This work aims to synthesize magnetic carbonaceous acids with high acidity and strong magnetism for biodiesel production from oils with high acid value. First, magnetic core is formed by hydrothermal precipitation from both glucose and iron chloride and subsequent high temperature pyrolysis. The core is again hydrothermally coated with glucose and stabilized by pyrolysis, and subsequent sulfonated as acid catalyst for *Jatropha* biodiesel production.

2. Experimental

2.1. Materials

Analytical reagents $FeCl_3{\cdot}6H_2O$ ($\geqslant$99.0%), glucose ($\geqslant$99.0%), urea ($\geqslant$99.0%), H_2SO_4 ($\geqslant$98.0%) and dehydrated methanol ($\geqslant$99.5%) were purchased from Xilong Chemical Factory Co., Ltd., (Shantou, Guangdong). Standard heptadecanoic acid methyl ester (HDAM; $C_{17:0}$) and other methyl esters [palmitate ($C_{16:0}$), linolenate ($C_{16:1}$), stearate ($C_{18:0}$), oleate ($C_{18:1}$), linoleate ($C_{18:2}$) and linolenate ($C_{18:3}$)] ($\geqslant$99.0%) were purchased from Sigma (Shanghai). Crude *Jatropha* oil (stored for five years) was obtained from our Garden in Xishuangbanna (Yunnan). According to the Chinese National standards (GBT 5530-2005 and 5534-2008), AV and saponification value (SV) of the crude *Jatropha* oil were measured by titration as 17.2 mg KOH/g and 195.7 mg KOH/g, respectively. So the molecular weight is 942.9 g/mol calculated by the formula [$M = (56.1 \times 1000 \times 3)/(SV - AV)$] [27].

2.2. Preparation of catalyst

A novel route with five steps by double hydrothermal precipitation and pyrolysis, as well as sulfonation was used for the catalyst synthesis:

(i and ii) magnetic core → (iii) magnetic carbon → (iv) carbonized magnetic carbon → (v) magnetic carbonaceous acid (catalyst). Detailed steps are described below:

2.2.1. Magnetic core (Fe/C) by hydrothermal precipitation and pyrolysis

Aqueous solution (300 mL) of $FeCl_3{\cdot}6H_2O$ (81.1 g), glucose (45.75 g) and solid urea (30.0 g) were loaded into an autoclave lined with ZrO_2 (500 mL; FCFD05-30, Jianbang Chemical Mechanical Co., Ltd., Yantai, Shandong). The vessel was sealed and heated to 180 °C (heating rate: 3.8 °C/min) for 14 h hydrothermal reaction with stirring (500 rpm) [24]. After reactions [$CO(NH_2)_2 + H_2O \rightarrow NH_3 + CO_2 + NH_4OH$;
$FeCl_3 + NH_4OH \rightarrow Fe(OH)_3 + NH_4Cl$; $Fe(OH)_3 \rightarrow Fe_2O_3 + H_2O$], solid products were recovered and washed thoroughly with deionized water and ethanol several times until reaching neutral solution, then dried in a freeze dryer (PDU-1200, EYELA, Tokyo Rikakikai Co., Ltd.) at −47 °C for 24 h. The solid sample was heated to 700 °C (heating rate: 7.4 °C/min) for 1.5 h pyrolysis in a tubular furnace (SGL-1100, Shanghai Daheng Optics and Fine Mechanics Co., Ltd.) under nitrogen flowing (200 mL/min) to form carbon-based magnetic core (Fe/C) by dehydration and reduction [$Fe(OH)_3 \rightarrow Fe_2O_3 + H_2O$; $Fe_2O_3 + C \rightarrow Fe_3O_4/Fe + CO/CO_2\uparrow$]. It was found that the magnetic core had very weak magnetism after sulfonated [Ms of 0.43 Am^2/kg with acid content of 1.67 mmol/g] due

Table 1
Comparison of acid content and magnetism of this work with other carbonaceous acid catalysts under different operation conditions.

Sample	Main raw materials	Operation conditions	Acid content (mmol/g)		Magnetism (Am^2/kg)	References
			NH_3-TPD analysis	Acid–base titration		
SO_3H–Fe/C	Glucose and $FeCl_3$	Hydrothermal precipitation: (180 °C, 14 h); pyrolysis: (700 °C, 1.5 h); sulfonation: (150 °C. H_2SO_4, 16 h)	1.67	–	0.43	This study
AC-600-SO_3H@Fe/C	Glucose and $FeCl_3$	Hydrothermal precipitation: (180 °C, 14 h); pyrolysis: (700 °C, 1.5 h); hydrothermal coating: (180 °C, 14 h); pyrolysis: (600 °C, 1.5 h); sulfonation: (150 °C. H_2SO_4, 16 h)	2.79 (1.0[a]; 3.7[b])	–	14.4	This study
Fe_3O_4@C-SO_3H	Glucose and $FeCl_3$	Hydrothermal carbonization: (Glucose 180 °C, 14 h); desiccation; (40 °C, 12 h); sulfonation: (60 °C. H_2SO_4, 24 h)	–	1.30	23	[24]
MLC-SO_3H	Enzymatic hydrolysis residue of corn stover and $FeCl_3$	Mixture: (300 rpm, 5 h); impregnation: (65 °C, 12 h); pyrolysis: (400 °C, 1 h); sulfonation: (150 °C. H_2SO_4, 10 h)	–	1.95	–	[25]
Sulfonated MCNAs	Xylene and ferrocene	Pyrolysis: (800 °C, the solution was injected by a syringe pump at a rate of 0.05 mL/min for 2 h with a flowrate of 60 sccm H_2 and 400 sccm Ar); sulfonation: (250 °C. H_2SO_4, 18 h)	0.38	–	6.32 (before sulfonation)	[26]

[a] By elemental analyzer.
[b] By EDX based on the calculation from the elemental composition of S.

to the dissolution of Fe_3O_4/Fe. So, it was re-coated with glucose in the next step.

2.2.2. Magnetic carbon (AC@Fe/C) by hydrothermal precipitation

The magnetic core was hydrothermally re-coated a carbonaceous layer with glucose to avoid leaching of Fe_3O_4/Fe during sulfonation. Fe/C powders (20 g), glucose (60 g) and H_2O (300 mL) were put into the above autoclave and heated to 180 °C for 14 h with stirring (500 rpm). After reactions, solid products were recovered by a permanent magnet (NeFeB, Ø37 mm × H18 mm), washed thoroughly with deionized water and ethanol several times until reaching neutral solution, dried in the freeze dryer at −47 °C for 24 h and an oven (WFO-710, EYELA, Tokyo Rikakikai Co., Ltd.) at 105 °C until reaching constant weight. The magnetic carbon was obtained and designated as AC@Fe/C.

2.2.3. Carbonized magnetic carbon (AC-T@Fe/C) by pyrolysis

In order to stabilize and restructure the magnetic carbon for sulfonation, it was heated to 400, 600 and 800 °C (heating rate: 4.1, 6.3 and 8.6 °C/min) for 1.5 h pyrolysis under nitrogen flowing (200 mL/min) in the tubular furnace to form carbonized magnetic carbons (designated as AC-T@Fe/C, *T* is pyrolysis temperature of 400, 600 and 800 °C) for sulfonation.

2.2.4. Magnetic carbonaceous acid (AC-T-SO_3H@Fe/C) by sulfonation

The carbonized magnetic carbon (AC-T@Fe/C) particles (10.0 g) and concentrated H_2SO_4 (98%, 200 mL) were added in a three-neck flask (500 mL) in oil bath (150 °C) for 16 h under nitrogen flowing (100 mL/min). The sulfonated samples were washed repeatedly with hot distilled water (80 °C) until reaching neutral solution, and hydrothermally pretreated at 200 °C (heating rate: 6 °C/min) for 3 h to remove SO_4^{2-} ions in the autoclave. After washed and dried in the freeze dryer at −47 °C for 24 h and the oven at 105 °C until reaching constant weight, the obtained catalysts (designated as AC-T-SO_3H@Fe/C) were ground and sieved by 200-mesh for biodiesel production.

2.3. Characterization

Synthesized carbonaceous particles (Fe/C, AC@Fe/C and AC-T@Fe/C) before and after sulfonation were analyzed by X-ray diffraction (XRD; Rigaku Rotaflex RAD-C, Tokyo) using a Cu Kα radiation source, and their morphologies were examined using scanning electron microscope (SEM; ZEISS EVO LS10, Cambridge, UK). Ms of samples was measured by a vibrating sample magnetometer (VSM; HH-15, Nanjing Nanda Instrument Plant, Jiangsu). Specific surface area and pore volume of samples were determined by Bruner Emmett and Teller (BET) method (Tristar II 3020, Micromeritics Instrument Co., Ltd., Northcross, GA). In the analysis, samples were degassed at 200 °C for 3 h and nitrogen with relative pressure of 0.05–0.985 was applied. The functional groups of catalysts were detected by Fourier transform-infrared spectroscopy (FT-IR; Nicolet iS10, Thermo Fisher Scientific Co., Ltd., Waltham, MA) over the range from 400 to 4000 cm^{-1} with a resolution of 0.4–4 cm^{-1} using the standard KBr disk method. Ammonia temperature programmed desorption (NH_3-TPD; Chemisorption analyzer, Quantachrome Instruments, Boynton Beach, FL) was used to assess their total acid density. In TPD analysis, sample (50–100 mg) was preheated to 400 °C at a heating rate of 5 °C/min to stabilize the catalyst and cooled to 50 °C exposed with He flowing (85 mL/min), and absorbed NH_3 by flushing NH_3 gas (10% NH_3 and 90% He, 85 mL/min) for 60 min. The sample was subsequently desorbed by heating to 400 °C at a heating rate of 5 °C/min and kept for 60–90 min with He flowing (85 mL/min). Four different volumes (0.5, 1, 1.5, 2 mL) of a standard NH_3 gas (10% NH_3 and 90% He) were used to calibrate total acid density. Thermal stability of catalysts (about 5 mg) was examined by thermo-gravimetric analysis (TGA; TA Q500 HiRes, T.A. Instruments, New Castle, DE). Temperature was ramped from 25 to 800 °C at 5 °C/min for data collection under He flowing (50 mL/min). Elemental compositions of catalysts were analyzed using an elemental analyzer (Vario EL III CHNS, Elementar Analysensysteme GmbH, Hanau, Germany). Synthesized particles, catalysts and biodiesel after carbonization were also analyzed to evaluate their elemental compositions or contaminants from catalysts by Energy-dispersive X-ray spectrometry (EDX; Quanta 200, Hillsboro, OR). It should be noted that the EDX data for elemental percentages are higher than actual values since H is not detectable and included.

2.4. Biodiesel production and analysis

Catalytic esterification and transesterification of crude *Jatropha* oil (about 18.6 g or 0.02 mol) without pretreatment with dehydrated methanol (methanol/oil molar ratio of 6/1–30/1) and catalyst (2.5–12.5 wt% of oil) were conducted in an autoclave with 50-mL quartz cup and 9.6-mL dead volume (YZPR-50, YanZheng Shanghai Experimental Instrument Co., Ltd.). The autoclave was sealed and pressurized with nitrogen to initial pressure of 2 MPa to avoid methanol evaporation to the dead volume at high temperature, and heated to 180–220 °C within 20–40 min under 750 rpm stirring. The actual reaction pressure in the reactor was 4.0 MPa at 180 °C and 6.5 MPa at 220 °C, that is much higher than the saturated methanol vapor pressure at corresponding temperature (e.g., 2.7 MPa at 180 °C and 5.8 MPa at 220 °C [28]). After reactions, catalyst was attracted on the wall of quartz cup by a magnet for 0.5–1 h (Fig. 1b) and liquid products were removed to a flask. The catalyst was washed by ethanol (20 mL) under magnetic stirring thoroughly (30 min) for 3–5 times, and dried at 105 °C until reaching a consistent weight. Recovery rate of catalyst was defined as:

$$\text{Recovery rate (wt\%)} = (\text{mass of recovered catalyst})/(\text{mass of fresh catalyst}) \times 100\% \quad (1)$$

Crude biodiesel in the flask at upper layer was filtered (pore size 0.22 μm) and analyzed by Gas Chromatography (GC; GC-2014, Shimadzu, Kyoto) with a capillary column of Rtx-Wax (30 m × Ø0.25 mm × 0.25 μm) under analytical conditions of column temperature 220 °C, injector temperature 260 °C, detector temperature 280 °C, carrier gas (He) with a flow rate 1 mL/min and split ratio 40/1. HDAM ($C_{17:0}$) was used as internal standard for quantitative analysis, according to the weights and GC peak areas of crude biodiesel and HDAM, biodiesel yield was calculated by equation:

$$\text{Biodiesel yield (wt\%)} = \{[(A_{C16:0}/f_{C16:0} + A_{C16:1}/f_{C16:1} + A_{C18:0}/f_{C18:0} + A_{C18:1}/f_{C18:1} + A_{C18:2}/f_{C18:2} + A_{C18:3}/f_{C18:3} + A_{\text{Cothers}})/A_{C17:0}] \times \text{weight of } C_{17:0}\}/(\text{weight of crude biodiesel}) \times 100\% \quad (2)$$

where f_{Cn} (1.014, 1.023, 1.076, 1.038, 1.019 and 0.926) (n = 16:0, 16:1, 18:0, 18:1, 18:2, 18:3) is the relative response factor of six standard methyl esters [palmitate ($C_{16:0}$), linolenate ($C_{16:1}$), stearate ($C_{18:0}$), oleate ($C_{18:1}$), linoleate ($C_{18:2}$) and linolenate ($C_{18:3}$)] to that of HDAM. It was separately calibrated for each GC peak in our previous work [29]. A_{Cn} is area for C_n peak. A_{Cothers} is area for other components except A_{Cn}.

3. Results and discussion

Photos for biodiesel production and catalyst separation in reaction quartz cup are showed in Fig. 1. Analytical results of XRD, VSM, SEM, BET, FT-IR, NH_3-TPD and TGA for synthesized particles and

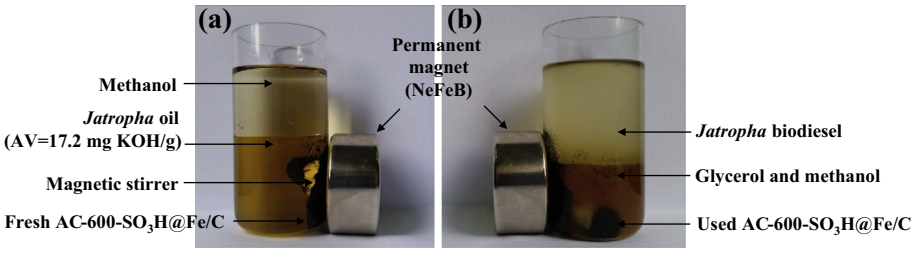

Fig. 1. Biodiesel production and catalyst separation in reaction quartz cup: (a) before and (b) after reaction.

catalysts are presented in Figs. 2–8, respectively. Table 1 compares acid content and magnetism of magnetic solid acids of this work with previous studies. Particle size of iron and iron oxides was calculated based on XRD data and listed in Table 2. Single-factor optimization, catalyst activity at different carbonized temperatures and catalyst cycles for biodiesel production from *Jatropha* oil with high AV (17.2 mg KOH/g) are given in Figs. 9–11. Element analysis of carbonized magnetic carbon (AC-600@Fe/C) and magnetic carbonaceous acid (AC-600-SO_3H@Fe/C) by EDX is demonstrated in supplemental materials (Fig. S1). Recycled catalysts were also analyzed by NH_3-TPD and results are illustrated in Figs. S2 and S3. EDX spectra of carbonized biodiesel (10 mL) catalyzed by magnetic carbonaceous acid (AC-600-SO_3H@Fe/C) are given in Fig. S4.

3.1. Characterization

3.1.1. XRD

In Fig. 2, the crystalline phases of Fe, Fe_3O_4, Fe_3C, Fe_2O_3 and aromatic carbon sheets are identified as compared with the cards from Joint Committee on Powder Diffraction Standards (JCPDS: 06-0696, 89-2355, 72-1110 and 39-1346) and Ref. [30]. The average particle size of Fe_3O_4 and Fe was calculated by Scherer equation [31]: $Dc = K\lambda/(\beta\cos\theta)$ (where Dc is the average particle size; K (0.89) is the Scherer constant; λ (0.1541 nm) is the X-ray wavelength of Cu Kα radiation; β is full-width at half-maximum; θ is the diffraction angle of the XRD reflection) (Table 2).

Fig. 2A shows that Fe/C and AC@Fe/C carbonaceous particles have well-crystallized Fe_3O_4 and Fe structures with characteristic and symmetric reflections, but the peak intensity of AC@Fe/C is much weaker due to a carbon layer coated. Fe_3O_4 particles have the same size in Fe/C and AC@Fe/C (29.5 nm) samples, but Fe particle size decreased from 53.1 nm in Fe/C to 42.5 nm in AC@Fe/C after coated hydrothermally.

In Fig. 2B, after carbonized at 400 °C, Fe_3O_4 and Fe crystals (in AC-400@Fe/C) changed little in characteristic reflections and particle size (Fig. 2B-a *vs.* Fig. 2A-b). As carbonized temperature rose from 400 to 600 and 800 °C (Fig. 2B-a, b and c), the diffraction peaks of Fe_3O_4 particles disappeared gradually, but Fe particle size increased from 42.5 to 106.3 nm then dipped to 70.8 nm. When temperature increased, Fe_3O_4 was reduced to Fe by carbon [$Fe_3O_4 + C \rightarrow Fe + CO_2/CO\uparrow$] at 600 °C [32], and further to Fe_3C particles [$Fe + C \rightarrow Fe_3C$] at 800 °C [33].

In Fig. 2C, after sulfonated, XRD spectra of magnetic carbonaceous acids (AC-T-SO_3H@Fe/C) change dramatically. Only a strong peak (for aromatic carbon sheet) remains if AC@Fe/C carbonized at 400 °C. At higher temperatures (Fig. 2C-b, 600 °C; Fig. 2C-c, 800 °C), additional Fe and Fe_2O_3 peaks appear because in concentrated H_2SO_4 solution, Fe was coated with dense oxidized Fe_2O_3 film [$Fe + H_2SO_4 \rightarrow Fe_2O_3 + H_2O + SO_2\uparrow$] that protected it from further corrosion. But, most of Fe_3O_4 and Fe_3C particles dissolved in H_2SO_4 solution (Fig. 2B *vs.* 2C). All sulfonated catalysts exhibit a broad and strong diffraction peak (at 2-Theta = 20–30°) for aromatic carbon sheets [30] due to the presence of amorphous carbons oriented in a random fashion [34]. But, the peak intensity declines gradually as the carbonized temperature rises from 400 to 800 °C (Fig. 2C-a, b and c). This may be due to that the carbonized magnetic carbons at low temperature (e.g., AC-400@Fe/C) with rich hydrogen and oxygen elements were easier to build aromatic carbon sheet structures when sulfonated in concentrated H_2SO_4 [34]. But, a portion of aromatic carbon sheet structures were formed at 800 °C (Fig. 2B-c) and inhibited concentrated H_2SO_4 to corrode carbon skeleton further [35].

3.1.2. VSM

Fig. 3A shows that Ms of the carbonized magnetic carbons is 23.5, 98.9 and 73.7 Am^2/kg at carbonized temperature of 400, 600 and 800 °C, respectively. This is because that Fe_3O_4 formed at 400 °C changed to Fe at 600 °C, and to Fe_3C at 800 °C as discussed above while Fe/Fe_3C has stronger magnetism than Fe_3O_4 [36] and Fe_3C has a lower Ms value than Fe [33]. So, AC-600@Fe/C has the strongest magnetism. After sulfonation, Ms decreased to 2.6, 14.4 and 11.1 Am^2/kg at carbonized temperature of 400, 600 and 800 °C, respectively (Fig. 3B) because of the dissolution of Fe_3O_4 and Fe_3C in concentrated H_2SO_4 solution. AC-600-SO_3H@Fe/C catalyst has the strongest magnetism because it contains the highest Fe (Fig. 2C-b *vs.* a and c).

3.1.3. SEM

In Fig. 4A-a, the magnetic core (Fe/C) is composed of porous particles (10–30 μm) agglomerated with tiny rough particles (<10 μm). After hydrothermally coated, they slightly grew to bigger particles agglomerated with smooth spheres (Fig. 4A-b). Little changed after the magnetic carbon (AC@Fe/C) carbonized at 400–800 °C (Fig. 4B). However, after sulfonation, the morphologies of magnetic carbonaceous acids (AC-T-SO_3H@Fe/C) changed dramatically for the carbonized magnetic carbon (AC-T@Fe/C) at low temperatures (400 and 600 °C). For example, catalyst AC-400-SO_3H@Fe/C became porous particles (Fig. 4C-a) from smooth spheres (Fig. 4B-a), but some spherical particles still remained for AC-600-SO_3H@Fe/C at higher carbonized temperature of 600 °C (Fig. 4C-b *vs.* Fig. 4B-b). When temperature rose to 800 °C, little morphology changed for AC-800-SO_3H@Fe/C catalyst (Fig. 4C-c *vs.* Fig. 4C-c). High carbonized temperature of 800 °C resulted in stable char structure to resist H_2SO_4 attack. At low pyrolysis temperatures of 400 and 600 °C, the carbon framework was flexible [35] to be corroded and dehydrated by H_2SO_4 during the sulfonation process.

3.1.4. BET

Nitrogen adsorption–desorption isotherms are given in Fig. 5. The carbonized magnetic carbon at 400 °C (AC-400@Fe/C) exhibits a very low adsorption capacity for nitrogen without clear hysteresis loop with pore volume of only 0.0063 cm^3/g and specific surface area of 4.28 m^2/g (Fig. 5A-a). It can be regarded it as nonporous amorphous carbon due to incomplete carbonization at 400 °C, and a large number of hydrogen and oxygen atoms still remained without the formation of porous structure [35]. As carbonized temperature increased to 600 °C (Fig. 5A-b), specific surface area rose

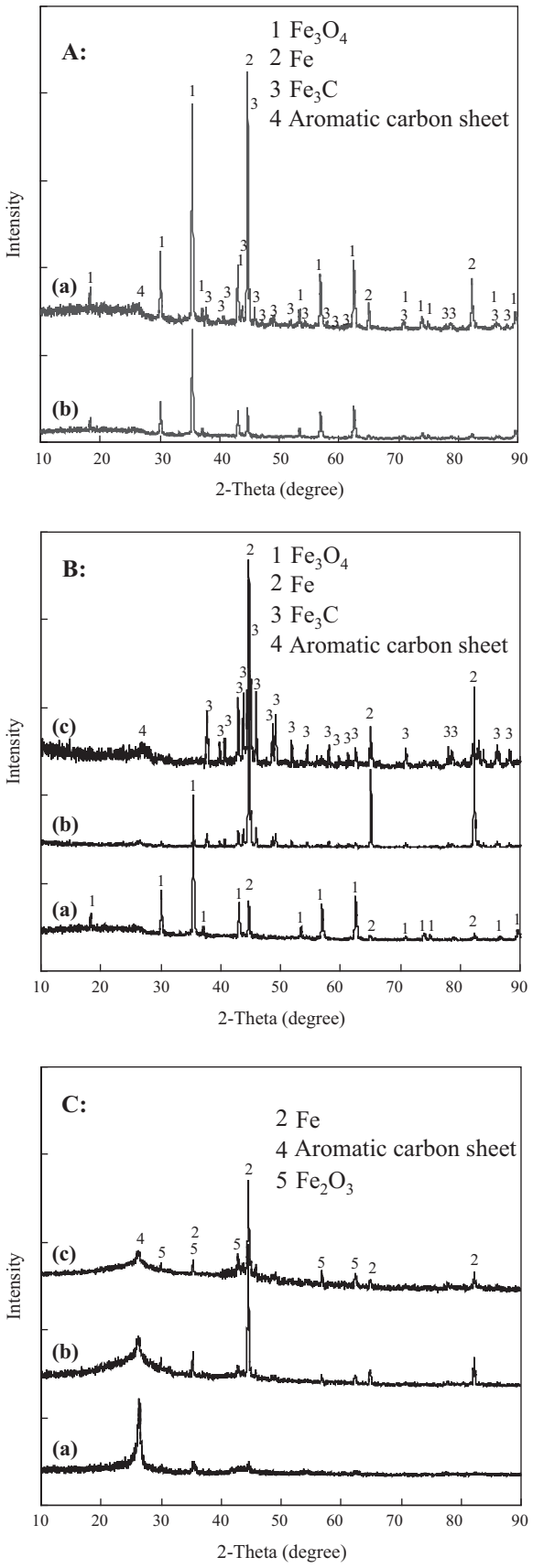

Fig. 2. XRD patterns of (A) magnetic core (a: Fe/C) and magnetic carbon (b: AC@Fe/C), (B) carbonized magnetic carbon (AC-T@Fe/C), and (C) magnetic carbonaceous acid (AC-T-SO_3H@Fe/C) (a: T = 400; b: T = 600; and c: T = 800).

to 36.5 m^2/g with larger pore volume (0.03 cm^3/g) due to numerous micro pore formation by removal of hydrogen and oxygen as volatile gases at 600 °C [37,38]. The generation of CO_2/CO in the reduction of Fe_3O_4 by carbon helped to create porous structures in AC-600@Fe/C [25]. At higher temperature of 800 °C (Fig. 5A-c), specific surface area jumped further to 56.3 m^2/g with pore volume of 0.12 cm^3/g due to deep degree pyrolysis and reduction reaction.

After sulfonation, both specific surface area and pore volume of magnetic carbonaceous acids (AC-T-SO_3H@Fe/C) rose with values of (218.5 m^2/g and 0.81 cm^3/g *vs.* 4.28 m^2/g and 0.0063 cm^3/g) at 400 °C, (88.9 m^2/g and 0.14 cm^3/g *vs.* 36.5 m^2/g and 0.03 cm^3/g) at 600 °C, and (57.3 m^2/g and 0.16 cm^3/g *vs.* 56.3 m^2/g and 0.12 cm^3/g) at 800 °C, respectively (Fig. 5B *vs.* A). The sharp increases for the sulfonated carbonaceous acid carbonized at 400 °C (but only slight rise at 800 °C) are due to that the unstable structure of carbonized magnetic carbon (AC-400@Fe/C) after incomplete pyrolysis was easily corroded and dehydrated by H_2SO_4 sulfonation to form micro porous particles with high surface area. On the other hand, the dissolution of Fe_3O_4 and Fe_3C particles also contributed the rising.

3.1.5. FT-IR

Fig. 6A shows the FT-IR spectra of magnetic carbons (AC-T@Fe/C) after carbonized at 400, 600 and 800 °C, respectively. All samples have absorptions at 1610 and 3460 cm^{-1} from O—H and C=O stretching vibration in phenolic —OH and —COOH groups generated during carbonization [25]. But, a strong absorption (Fig. 6A-a) at 560 cm^{-1} for AC-400@Fe/C from Fe—O stretching vibration in Fe_3O_4 [25] gradually disappeared due to its reduction to Fe and Fe_3C at high temperatures of 600 and 800 °C (Fig. 6A-b, c) as discussed in the above Section 3.1.1 XRD (Fig. 2B).

After sulfonation (Fig. 6B), all samples have absorptions at 1060 and 1180 cm^{-1} from C—O—S and O=S=O stretching vibration in —SO_3H groups [25]. The absorption at 1640 cm^{-1} is from C=C stretching vibration in aromatic carbons. The absorption at 560 cm^{-1} for Fe—O stretching vibration in AC-400-SO_3H@Fe/C disappeared (Fig. 6B-a), but appeared in AC-600-SO_3H@Fe/C and AC-800-SO_3H@Fe/C. This is because that Fe_3O_4 in AC-400 @Fe/C dissolved during sulfonation, but Fe_2O_3 was formed from Fe in the catalysts carbonized at 600 and 800 °C by oxidation of Fe in concentrated H_2SO_4 as confirmed by XRD analysis (Fig. 2C).

AC-600@Fe/C before and after sulfonation was analyzed by EDX (Fig. S1), the spectra revealed that S content dramatically increased from <0.3 wt% to <12.2 wt% after sulfonation, indicating that —SO_3H groups were successfully incorporated into the carbonized magnetic carbon. The trace amount of S before sulfonation for AC-600@Fe/C was possibly from the contaminated S compounds remained in autoclave.

3.1.6. TPD

Total acid density of magnetic carbonaceous acids (AC-T-SO_3H@Fe/C) was determined by NH_3-TPD analysis (Fig. 7).

For carbonized magnetic carbons (Fig. 7A), a major desorption peak at 135 °C appeared for AC-400@Fe/C (total acid density 0.12 m mol/g) from incompletely formed carbon sheets with weak acid sites (—OH and —COOH) [17]. Total acid density rose to 0.27 mmol/g for AC-600@Fe/C when carbonized temperature grew to 600 °C due to its larger specific surface area and pore volume (36.5 m^2/g *vs.* 4.28 m^2/g) and (0.03 cm^3/g *vs.* 0.0063 cm^3/g) (Fig. 7A-b *vs.* a) with more acid sites exposed on the surface and inner wall [39,40]. However, total acid density dropped to only 0.05 mmol/g for AC-800@Fe/C because less acid sites or hydrogen and oxygen elements remained at 800 °C [22,37] even though it had high specific surface area and pore volume.

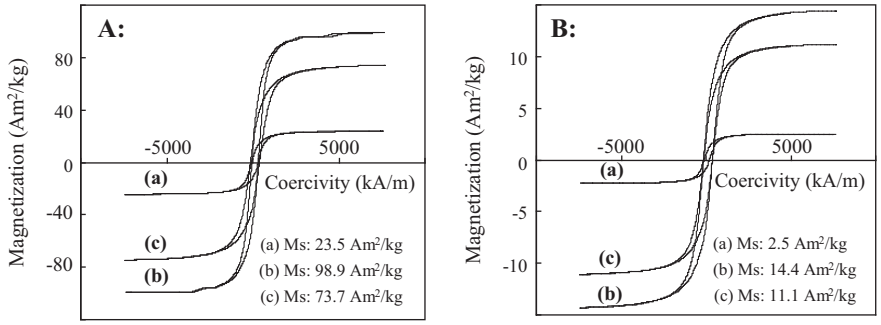

Fig. 3. Hysteresis loops of (A) carbonized magnetic carbon (AC-T@Fe/C) and (B) magnetic carbonaceous acid (AC-T-SO_3H@Fe/C) (a: T = 400; b: T = 600; and c: T = 800).

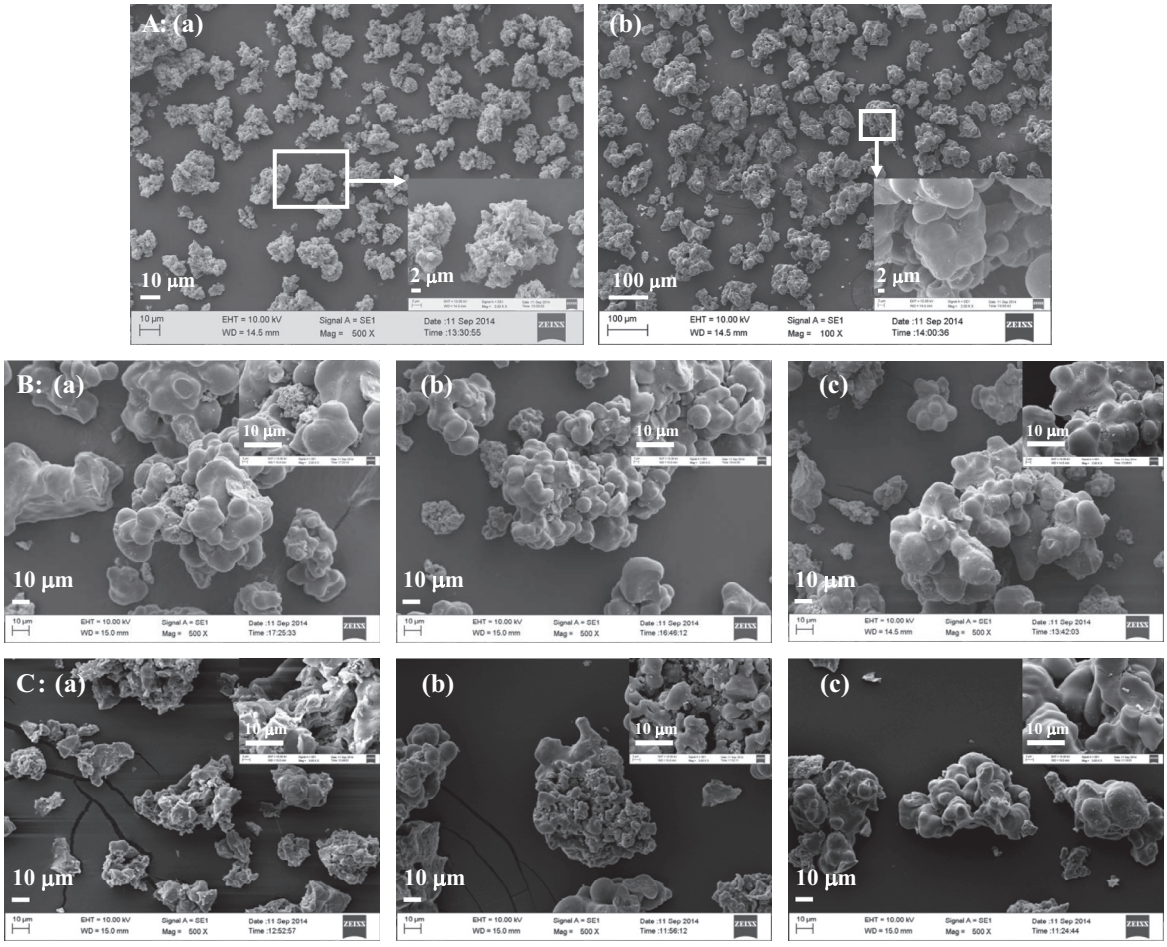

Fig. 4. SEM images of (A) magnetic core (a: Fe/C) and magnetic carbon (b: AC@Fe/C), (B) carbonized magnetic carbon (AC-T@Fe/C), and (C) magnetic carbonaceous acid (AC-T-SO_3H@Fe/C) (a: T = 400; b: T = 600; and c: T = 800).

After sulfonation (Fig. 7B), 2–3 major desorption peaks are observed at 50–400 °C for the catalysts, and total acid density rises more than 10 times [(3.26 *vs.* 0.12 mmol/g) at 400 °C, (2.79 *vs.* 0.27 mmol/g) at 600 °C, (1.24 *vs.* 0.05 mmol/g) at 800 °C] because of the presence of active group (—SO_3H). The sulfonated carbonaceous catalysts have high total acid density when they were carbonized at low temperatures (400 and 600 °C), but have a very low value at 800 °C. This is because many hydrogen and oxygen atoms still remained in the catalysts when carbonized at 400 and 600 °C, to attach —SO_3H group [37] but the formed aromatic carbon sheet at 800 °C in AC-800@Fe/C (Fig. 2B-c) inhibited the attachment [35]. Elemental compositions of AC-600-SO_3H@Fe/C were also analyzed and showed an increase in S content (3.2 S, 63.6 C, 2.3 H and 1.1 wt% N *vs.* 0.2 S, 59.1 C, 2.0 H and 1.8 wt% N before sulfonation) with its sulfuric acid density (—SO_3H) increased from 0.06 to 1.0 mmol/g calculated based on S content. EDX spectrum reveals a high S content of 12.2% (Fig. S1b), if including 2% H, the S content is about 12% (or 3.7 mmol/g sulfuric acid density) that is much higher than 3.2% obtained by elemental analyzer. These results demonstrate that the re-coated carbon layer on the surface has a much higher acid density because it has more functional groups and chance to bond —SO_3H than the magnetic core.

Since AC-600-SO_3H@Fe/C catalyst has the strongest magnetism (Ms: 14.4 Am^2/kg) with high total acid density (2.79 mmol/g), it is selected for biodiesel production in next section. As compared to other magnetic carbonaceous acids in previous works (Table 1),

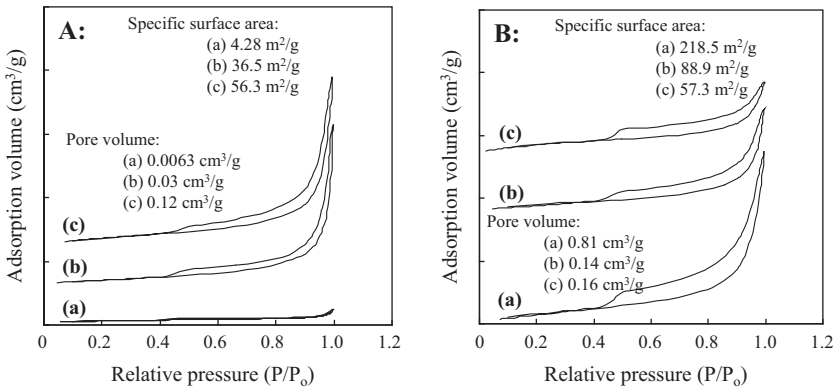

Fig. 5. Nitrogen adsorption/desorption isotherms of (A) carbonized magnetic carbon (AC-T@Fe/C) and (B) magnetic carbonaceous acid (AC-T-SO_3H@Fe/C) (a: T = 400; b: T = 600; and c: T = 800).

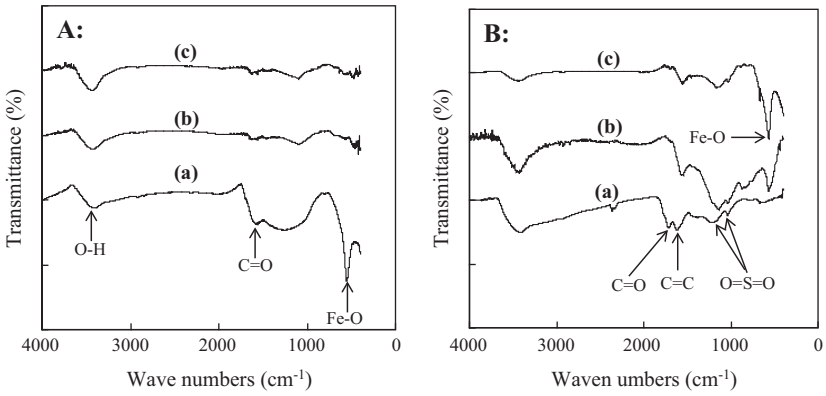

Fig. 6. FT-IR spectra of (A) carbonized magnetic carbon (AC-T@Fe/C) and (B) magnetic carbonaceous acid (AC-T-SO_3H@Fe/C) (a: T = 400, b: T = 600, and c: T = 800).

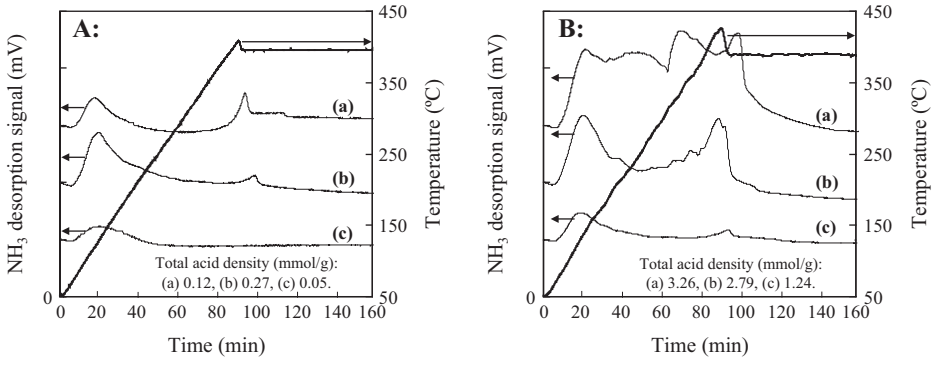

Fig. 7. NH_3-TPD curves of (A) carbonized magnetic carbon (AC-T@Fe/C) and (B) magnetic carbonaceous acid (AC-T-SO_3H@Fe/C) (a: T = 400; b: T = 600; and c: T = 800).

such as Fe_3O_4@C-SO_3H [24], MLC-SO_3H [25] and sulfonated MCNAs [26], AC-600-SO_3H@Fe/C catalyst has the highest acid content (2.79 *vs.* 1.3, 1.95 and 0.38 mmol/g) with strong magnetism. Even though, Fe_3O_4@C-SO_3H has the higher Ms (23 Am^2/kg) but its acid content is too low (1.3 mmol/g) because of its low sulfonated temperature than AC-600-SO_3H@Fe/C (60 °C *vs.* 150 °C).

In the above TPD results, catalysts were stabilized *via* thermal pretreatment by heating to 400 °C with He flowing, they may be decomposed before NH_3 absorption. Therefore, thermal stability of AC-600-SO_3H@Fe/C catalyst was analyzed by TGA. In Fig. 8A, it is found that a minor weight loss (about 7.0 wt%) at 25–200 °C from the release of water and gases [34], and a very slight thermal decomposition at 200–400 °C (2.0 wt% of weight loss) probably from polycyclic aromatic hydrocarbons bonded to sulfuric groups. So, an additional TPD analysis was conducted for AC-600-SO_3H@Fe/C without thermal pretreatment (Fig. 8B), a slight higher total acid density (3.05 *vs.* 2.79 mmol/g) was obtained (datum of 0.32 for a blank run without adsorption of NH_3 was subtracted, Fig. 8B-a). The total acid density data analyzed in this work may present smaller slightly.

3.2. Jatropha biodiesel production with AC-600-SO_3H@Fe/C

Variables of catalyst dosage (2.5–12.5 wt% of oil), methanol/oil molar ratio (6/1–30/1), reaction temperature (180–220 °C) and reaction time (2.5–12.5 h, excluding heating and cooling times)

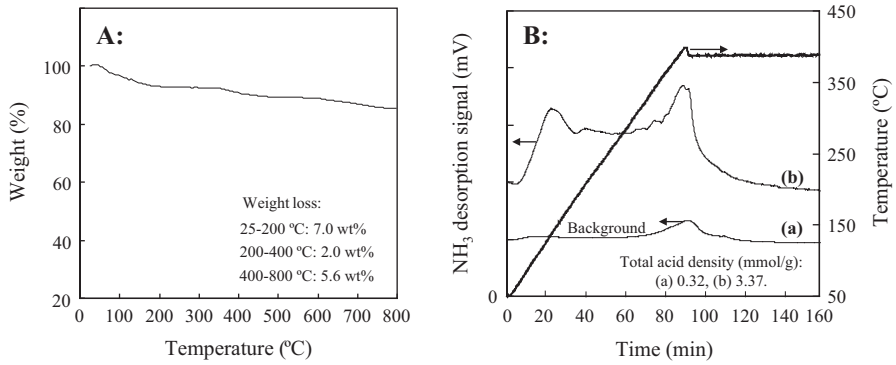

Fig. 8. (A) TGA and (B) NH_3-TPD curves of AC-600-SO_3H@Fe/C catalyst without thermal pretreatment at 400 °C (a: a blank ran without adsorption of NH_3 as background).

Table 2
Average particle size of Fe_3O_4 and Fe crystals calculated by Scherer equation: $Dc = K\lambda/(\beta\cos\theta)$ (θ for Fe_3O_4 is 35.46°/2 × 3.14/180 = 0.31, and for Fe is 44.74°/2 × 3.14/180 = 0.39).

No.	Sample	Crystalline phase	β	Particle size (nm)
Fig. 2A-a	Fe/C	Fe_3O_4	0.28° × 3.14/180 = 0.0049	29.5
		Fe	0.16° × 3.14/180 = 0.0035	53.1
Fig. 2A-b	AC@Fe/C	Fe_3O_4	0.28° × 3.14/180 = 0.0049	29.5
		Fe	0.2° × 3.14/180 = 0.0035	42.5
Fig. 2B-a	AC-400@Fe/C	Fe_3O_4	0.28° × 3.14/180 = 0.0049	29.5
		Fe	0.2° × 3.14/180 = 0.0035	42.5
Fig. 2B-b	AC-600@Fe/C	Fe_3O_4	–	–
		Fe	0.12° × 3.14/180 = 0.0021	106.3
Fig. 2B-c	AC-800@Fe/C	Fe_3O_4	–	–
		Fe	0.08° × 3.14/180 = 0.0014	70.8

were studied for the esterification and transesterification of *Jatropha* oil with high AV (17.2 mg KOH/g) to biodiesel by single factor test. Two repeated experiments were done for each run and the reported biodiesel yields were averaged data with standard deviation (σ) of 0.8–4.2% (Fig. 9). The initial conditions set below for optimization are referred to the previous results (catalyst of 5 wt%, methanol/oil molar ratio of 12/1, reaction temperature of 220 °C and reaction time of 5 h) [23].

3.2.1. Catalyst dosage

Catalyst from 2.5 wt% to 12.5 wt% was applied for biodiesel production under conditions of 220 °C for 5 h with 12/1 methanol/oil molar ratio. In Fig. 9a, biodiesel yield jumped sharply from 65.5% to 80.3% as catalyst rose from 2.5 wt% to 5 wt%, and increased gradually to the highest yield of 85.1% at 10 wt% catalyst. However, as catalyst grew further from 10 wt% to 12.5 wt%, biodiesel yield dropped slightly from 85.1% to 83.6%. This was possibly due to

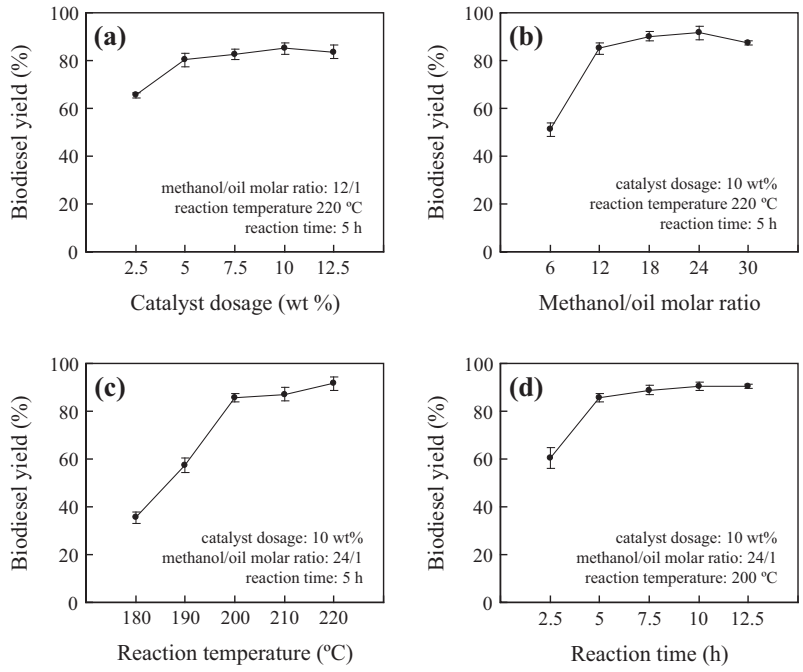

Fig. 9. Single-factor optimization of biodiesel production from *Jatropha* oil (AV = 17.2 mg KOH/g) with AC-600-SO_3H@Fe/C magnetic acid catalyst: (a) catalyst dosage, (b) methanol/oil molar ratio, (c) reaction temperature, and (d) reaction time.

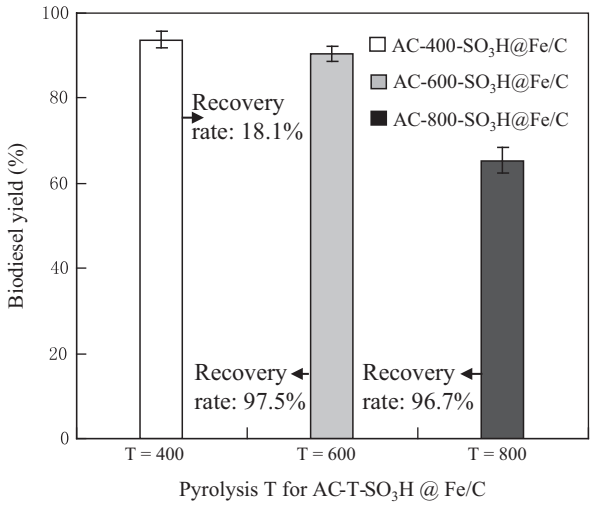

Fig. 10. *Jatropha* biodiesel yield changed with pyrolysis temperature for AC-T-SO_3H@Fe/C catalyst (Reaction conditions: 200 °C for 10 h with 24/1 methanol/oil molar ratio and 10 wt% catalyst).

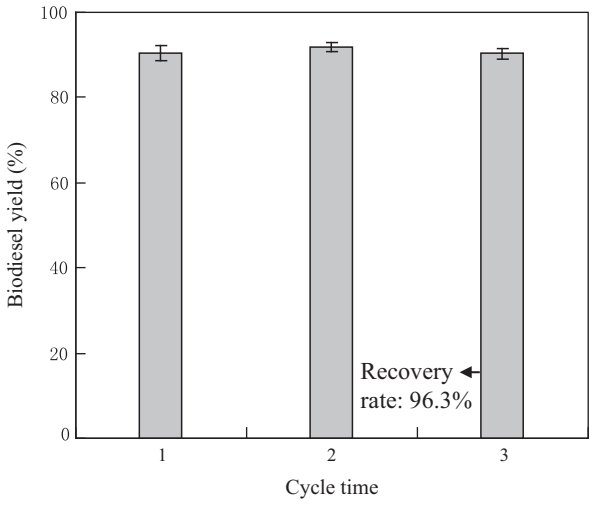

Fig. 11. Catalyst (AC-600-SO_3H@Fe/C) cycles for the *Jatropha* biodiesel production (Reaction conditions: 200 °C for 10 h with 24/1 methanol/oil molar ratio and 10 wt% catalyst).

the difficult mixing of liquid reactants with high concentration of magnetic carbonaceous catalyst under magnetic stirring. So, 10 wt% catalyst is selected as the best value for the next experiments.

3.2.2. Methanol/oil molar ratio

Theoretical methanol/oil molar ratio for the transesterification of triglycerides is 3/1. High methanol/oil molar ratio from 6/1 to 30/1 was required in this work under 220 °C for 5 h with 10 wt% catalyst because of the evaporation of methanol to the dead volume of the autoclave at high temperature (Fig. 9b). When methanol/oil molar ratio grew from 6/1 to 12/1, biodiesel yield rose sharply from 51.1% to 85.1%, and gradually increased to 90.2% and the maximum of 91.6% at molar ratio of 18/1 and 24/1, respectively. But, the yield dropped slightly to 87.5% at molar ratio of 30/1 owing to the relative low concentration of catalyst in the reaction system caused by excess methanol. So, 24/1 methanol/oil molar ratio is selected as the best value for the following experiments.

3.2.3. Reaction temperature

Five different temperatures from 180 to 220 °C were selected for biodiesel production with 10 wt% catalyst, 24/1 methanol/oil molar ratio and 5 h reaction time (Fig. 9c). A big increase in biodiesel yield (85.6% *vs.* 35.5%) occurred from 180 to 200 °C, and the yield rose slowly to 87.2% at 210 °C and 91.6% at 220 °C, respectively. High temperature resulted in high biodiesel yield, but the active group is easily leached. So, 200 °C is selected as the best value.

3.2.4. Reaction time

Reaction time from 2.5 to 12.5 h was chosen for biodiesel production under conditions of 10 wt% catalyst, 24/1 methanol/oil molar ratio and 200 °C temperature (Fig. 9d). When time rose from 2.5 to 5 h, biodiesel yield increased from 60.5% to 85.6% sharply, and gradually rose to 88.8%, 90.5% and 90.6% at 7.5, 10 and 12.5 h, respectively. Since little increased for biodiesel yield from 10 to 12.5 h, the best value for reaction time is selected as 10 h.

In conclusion, the best conditions for *Jatropha* biodiesel production with 90.5% biodiesel yield were selected as: 10 wt% catalyst, 24/1 methanol/oil molar ratio, 200 °C temperature and 10 h reaction time. Under the conditions, catalyst recovery and recycles are studied in next section.

3.2.5. Catalyst recovery and recycles

Under the above best conditions, the three synthesized catalysts (AC-T-SO_3H@Fe/C; T = 400, 600 and 800) were tested to catalyze biodiesel production (Fig. 10). Biodiesel yields were 92.7%, 90.5% and 65.4% with catalysts carbonized at 400, 600 and 800 °C, that were corresponding to their total acid densities of 3.26, 2.79 and 1.24 mmol/g, respectively. After first-used, the catalysts (AC-T-SO_3H@Fe/C; T = 400, 600 and 800) were recovered by a magnet with recovery rate of 18.1%, 97.5% and 96.7%, that was corresponding to their magnetisms (Ms) of 2.5, 14.4 and 11.1 Am^2/kg, respectively. TPD analysis shows that total acid density was reduced to 2.17, 2.52 and 1.03 mmol/g for the first-used catalysts carbonized at 400, 600 and 800 °C, respectively (Fig. S2). These experimental results show that AC-600-SO_3H@Fe/C is the best catalyst for *Jatropha* biodiesel production as we supposed before for its excellent performance in recovery rate and stability.

Recycle experiments were conducted for AC-600-SO_3H@Fe/C catalyst (Fig. 11). Little biodiesel yield changed for three cycles (90.5%, 91.8%, 90.3%) with high catalyst recovery rate of 96.3% after 3 cycles due to only a slight reduction in total acid density (from 2.79 to 2.43 mmol/g) (Fig. S3).

Biodiesels from the three cycles were analyzed their AV by titration with values of 0.12, 0.09 and 0.13 mg KOH/g that are lower than the value (0.5 mg KOH/g) for US national standard [41]. The three biodiesels (10 mL) were carbonized at 700 °C, and analyzed by EDX and found they were composed of C and O (H undetectable) without any Fe and other elements contaminated from the catalyst in the three cycles (Fig. S4).

3.3. Applications

For biodiesel production from high AV cooking oil (12 mg KOH/g), Zhang et al. [42,43] compared two main conventional methods [one-step acid-catalyzed with H_2SO_4 at 80 °C *vs.* two-step alkali-catalyzed after acid-pretreatment (esterification with H_2SO_4 at 70 °C, and transesterification with NaOH at 60 °C) processes] on a commercial scale. Economic assessment and sensitivity analysis showed that the one-step process proved to be technically feasible with less complexity (such as without pretreatment unit for esterification reactor, glycerol washing tower and methanol recovery process) than the two-step process. So, one-step process is a competitive alternative to commercial biodiesel production by the alkali-catalyzed process (e.g., 644 *vs.* 884

$/tonne of break-even price of biodiesel) [43]. However, liquid acid H_2SO_4 is hard to recover and usually requires neutralization.

In this work, one-step process was also used to produce biodiesel in the presence of the synthesized magnetic carbonaceous acid directly from low-qualified oils with high AV (17.2 mg KOH/g) without pretreatment. After reactions, the biodiesel contains high fatty acid methyl esters (FAMEs; 90–92% purity or biodiesel yield) and low AV (⩽0.13 mg KOH/g) without any pollutants from catalysts. The solid catalyst can be recovered easily by external magnetic field for recycles and is less corrosive to reactors than liquid acid (e.g., H_2SO_4). However, biodiesel with 90–92% purity of FAMEs may have to be re-transesterified or blended with less portion to fossil diesel to achieve the international standards for biodiesel [44]. Another disadvantage of this process is that reaction conditions are under severe conditions (e.g., 220 °C and 6.5 MPa) as compared to the method with solid base catalysts (e.g., 94.9% biodiesel yield at 65 °C with Na_2SiO_3 [27]). Therefore, further study is required to improve the catalyst activity for transesterification by loading strong base sites to become a bifunctional catalyst with both acidic and basic properties.

On the other hands, with the strong acidity, the catalyst can find applications in the esterification of FFAs from crude oils for pretreatment at low temperatures (e.g., <100 °C [23]) and the hydrolysis of lignocelluloses under mild conditions (e.g., 140 °C [24]).

4. Conclusions

A novel route with five steps by hydrothermal, pyrolysis and sulfonation processes was developed to synthesize a novel carbonaceous acid with high acid density and strong magnetism. For the magnetic core (Fe/C) synthesized by hydrothermal precipitation and pyrolysis, it is necessary to re-coat a carbonaceous layer to protect Fe_3O_4/Fe from leaching during sulfonation. Before sulfonation, the magnetic carbon (AC@Fe/C) needs pyrolysis step to achieve a suitable structure to load —SO_3H group and avoid leaching Fe_3O_4/Fe. It was found that pyrolysis temperature at 600 °C led to excellent structure to produce catalyst (AC-600-SO_3H@Fe/C) with high acid density (2.79 mmol/g) and strong magnetism (14.4 Am^2/kg). The catalyst presents high active, stable and recoverable in the production of *Jatropha* biodiesel with high yields for 3 cycles (90.5%, 91.8%, 90.3%), slight reduction in total acid density (2.43 *vs.* 2.79 mmol/g) and high catalyst recovery rate of 96.3%.

Acknowledgements

The authors wish to acknowledge the financial support from Chinese Academy of Sciences [CAS 135 program (XTBG-T02) and equipment R&D grant (No. YZ201260)], the Yunnan Provincial Government (Baiming Haiwai Gaocengci Rencai Jihua), and the Natural Science Foundation of China (No. 31400518). Thanks are also given to the Central Laboratory of Xishuangbanna Tropical Botanical Garden for SEM analysis, and Dr. Lin Lin, Miss Wenyu Wu and Mr. Chunyu Sun (Jiangsu University) for VSM analysis.

Appendix A. Supplementary material

Supplementary data associated with this article can be found, in the online version, at http://dx.doi.org/10.1016/j.apenergy.2015.06.044.

References

[1] Jacobson MZ. Review of solutions to global warming, air pollution, and energy security. Energy Environ Sci 2009;2:148–73.
[2] Sathre R. Comparing the heat of combustion of fossil fuels to the heat accumulated by their lifecycle greenhouse gases. Fuel 2014;115:674–7.
[3] Lois E. Definition of biodiesel. Fuel 2007;86:1212–3.
[4] Lin L, Zhou CS, Saritporn V, Shen XQ, Dong MD. Opportunities and challenges for biodiesel fuel. Appl Energy 2011;88:1020–31.
[5] Tang Y, Meng M, Zhang J, Lu Y. Efficient preparation of biodiesel from rapeseed oil over modified CaO. Appl Energy 2011;88:2735–9.
[6] Gao L, Wang S, Xu W, Xiao G. Biodiesel production from palm oil over monolithic KF/γ-Al_2O_3/honeycomb ceramic catalyst. Appl Energy 2015;146:196–201.
[7] Long YD, Fang Z, Su TC, Yang Q. Co-production of biodiesel and hydrogen from rapeseed and Jatropha oils with sodium silicate and Ni catalysts. Appl Energy 2014;113:1819–25.
[8] Deng X, Fang Z, Liu YH. Ultrasonic transesterification of Jatropha curcas L. oil to biodiesel by a two-step process. Energy Convers Manage 2010;51:2802–9.
[9] Shu Q, Gao J, Nawaz Z, Liao Y, Wang D, Wang J. Synthesis of biodiesel from waste vegetable oil with large amounts of free fatty acids using a carbon-based solid acid catalyst. Appl Energy 2010;87:2589–96.
[10] Fu J, Chen L, Lv P, Yang L, Yuan Z. Free fatty acids esterification for biodiesel production using self-synthesized macroporous cation exchange resin as solid acid catalyst. Fuel 2015;154:1–8.
[11] Talebian-Kiakalaieh A, Amin NAS, Zarei A, Noshadi I. Transesterification of waste cooking oil by heteropoly acid (HPA) catalyst: optimization and kinetic model. Appl Energy 2013;102:283–92.
[12] Kiss AA, Dimian AC, Rothenberg G. Solid acid catalysts for biodiesel production – towards sustainable energy. Adv Synth Catal 2006;348:75–81.
[13] Furuta S, Matsuhashi H, Arata K. Catalytic action of sulfated tin oxide for etherification and esterification in comparison with sulfated zirconia. Appl Catal 2004;269:187–91.
[14] Furuta S, Matsuhashi H, Arata K. Biodiesel fuel production with solid superacid catalysis in fixed bed reactor under atmospheric pressure. Catal Commun 2004;5:721–3.
[15] Ezebor F, Khairuddean M, Abdullah AZ, Boey PL. Esterification of oily-FFA and transesterification of high FFA waste oils using novel palm trunk and bagasse-derived catalysts. Energy Convers Manage 2014;88:1143–50.
[16] Kulkarni MG, Gopinath R, Meher LC, Dalai AK. Solid acid catalyzed biodiesel production by simultaneous esterification and transesterification. Green Chem 2006;45:2901–13.
[17] Huang CC, Chen HM, Chen CH, Huang JC. Effect of surface oxides on hydrogen storage of activated carbon. Sep Purif Technol 2010;70:291–5.
[18] Díaz JA, Akhavan H, Romero A, Garcia-Minguillan AM, Romero R, Giroir-Fendler A, et al. Cobalt and iron supported on carbon nanofibers as catalysts for Fischer–Tropsch synthesis. Fuel Process Technol 2014;128:417–24.
[19] Santos A, Yustos P, Rodriguez S, Garcia-Ochoa F. Wet oxidation of phenol, cresols and nitrophenols catalyzed by activated carbon in acid and basic media. Appl Catal B – Environ 2006;65:269–81.
[20] Ji J, Zhang G, Chen H, Wang S, Zhang G, Zhang F, et al. Sulfonated graphene as water-tolerant solid acid catalyst. Chem Sci 2011;2:484–7.
[21] Kanbur Y, Küçükyavuz Z. Synthesis and characterization of surface modified fullerene. Fuller Nanotu Car N 2012;2:119–26.
[22] Peng F, Zhang L, Wang H, Lv P, Yu H. Sulfonated carbon nanotubes as a strong protonic acid catalyst. Carbon 2005;43:2405–8.
[23] Pua FL, Fang Z, Zakaria S, Chia CH, Guo F. Direct production of biodiesel from high-acid value *Jatropha* oil with solid acid catalyst derived from lignin. Biotechnol Biofuels 2011;4:56–64.
[24] Zhang C, Wang H, Liu F, Wang L, He H. Magnetic core-shell Fe_3O_4@C-SO_3H nanoparticle catalyst for hydrolysis of cellulose. Cellulose 2013;20:127–34.
[25] Hu L, Tang X, Wu Z, Lin L, Xu J, Xu N, et al. Magnetic lignin-derived carbonaceous catalyst for the dehydration of fructose into 5-hydroxymethylfurfural in dimethylsulfoxide. Chem Eng J 2015;263:299–308.
[26] Liu Z, Fu X, Tang S, Cheng Y, Zhu L, Xing L, et al. Sulfonated magnetic carbon nanotube arrays as effective solid acid catalysts for the hydrolyses of polysaccharides in crop stalks. Catal Commun 2014;56:1–4.
[27] Zhang F, Fang Z, Wang YT. Biodiesel production directly from oils with high acid value by magnetic Na_2SiO_3@Fe_3O_4/C catalyst and ultrasound. Fuel 2015;150. 377-7.
[28] Lemmon EW, Huber ML, McLinden MO. NIST reference fluid thermodynamic and transport properties-REFPROP; 2002.
[29] Xue BJ, Luo J, Zhang F, Fang Z. Biodiesel production from soybean and *Jatropha* oils by magnetic $CaFe_2O_4$–$Ca_2Fe_2O_5$-based catalyst. Energy 2014;68:584–91.
[30] Nakajima K, Hara M. Environmentally benign production of chemicals and energy using a carbon-based strong solid acid. J Am Ceram Soc 2007;90:3725–34.
[31] Liu XR. Catalyst characterization and evaluation. In: Huang ZT, editor. Handbook of Industrial Catalyst. Beijing: Chemical Industry Press; 2004. p. 187–9 [in Chinese].
[32] Pereira MC, Coelho FS, Nascentes CC, Fabris JD, Araújo MH, Sapag K, et al. Use of activated carbon as a reactive support to produce highly active-regenerable Fe-based reduction system for environmental remediation. Chemosphere 2010;81:7–12.
[33] Fei Y, Brosh E. Experimental study and thermodynamic calculations of phase relations in the Fe–C system at high pressure. Earth Planet Sci Lett 2014;408:155–62.
[34] Dawodu FA, Ayodele O, Xin J, Zhang S, Yan D. Effective conversion of non-edible oil with high free fatty acid into biodiesel by sulphonated carbon catalyst. Appl Energy 2014;114:819–26.

[35] Wang L, Dong X, Jiang H, Li G, Zhang M. Preparation of a novel carbon-based solid acid from cassava stillage residue and its use for the esterification of free fatty acids in waste cooking oil. Bioresour Technol 2014;158:392–5.
[36] López de Arroyabe Loyo R, Nikitenko SI, Scheinost AC, Simonoff M. Immobilization of selenite on Fe_3O_4 and Fe/Fe_3C ultrasmall particles. Environ Sci Technol 2008;42:2451–6.
[37] Anderson JM, Johnson RL, Schmidt-Rohr K, Shanks BH. Solid state NMR study of chemical structure and hydrothermal deactivation of moderate-temperature carbon materials with acidic SO_3H sites. Carbon 2014;74:333–45.
[38] Hara M, Yoshida T, Takagaki A, Takata T, Kondo JN, Hayashi S, et al. A carbon material as a strong protonic acid. Angew Chem Int Ed 2004;43:2955–8.
[39] Shu Q, Nawaz Z, Gao J, Liao Y, Zhang Q, Wang D, et al. Synthesis of biodiesel from a model waste oil feedstock using a carbon-based solid acid catalyst: reaction and separation. Bioresour Technol 2010;101:5374–84.
[40] Shu Q, Zhang Qiang, Xu G, Nawaz Z, Wang D, Wang J. Synthesis of biodiesel from cottonseed oil and methanol using a carbon-based solid acid catalyst. Fuel Process Technol 2009;90:1002–8.
[41] ASTM D6751-07b. Standard Specification for Biodiesel Fuel Blend Stock (B100) for Middle Distillate Fuels, ASTM International, West Conshohocken, PA; 2007 <www.astm.org>.
[42] Zhang Y, Dube MA, McLean DD, Kates M. Biodiesel production from waste cooking oil: 1. Process design and technological assessment. Bioresour Technol 2003;89:1–15.
[43] Zhang Y, Dube MA, McLean DD, Kates M. Biodiesel production from waste cooking oil: 2. Economic assessment and sensitivity analysis. Bioresour Technol 2003;90:229–40.
[44] Oguma M, Lee YJ, Goto S. An overview of biodiesel in Asian countries and the harmonization of quality standards. Int J Automot Technol 2012;13:33–41.